

# Therapeutic Evaluation of Epstein-Barr Virus-encoded Latent Membrane Protein-1 Targeted DNAzyme for Treating of Nasopharyngeal Carcinomas

Ya Cao<sup>1</sup>, Lifang Yang<sup>1</sup>, Wuzhong Jiang<sup>2</sup>, Xiaoyi Wang<sup>3</sup>, Weihua Liao<sup>3</sup>, Guolin Tan<sup>4</sup>, Yuping Liao<sup>2</sup>, Yuanzheng Qiu<sup>5</sup>, Deyun Feng<sup>6</sup>, Faqing Tang<sup>7</sup>, Bob L Hou<sup>8</sup>, Ling Zhang<sup>2</sup>, Jia Fu<sup>2</sup>, Fengjiao He<sup>2</sup>, Xiaoyu Liu<sup>3</sup>, Wenjuan Jiang<sup>2</sup>, Tubao Yang<sup>9</sup> and Lun-Quan Sun<sup>10</sup>

<sup>1</sup>Cancer Research Institute and Key laboratory of Ministry of Education, Central South University, Changsha, China; <sup>2</sup>Department of Oncology, Xiangya Hospital, Central South University, Changsha, China; <sup>3</sup>Department of Radiology, Xiangya Hospital, Central South University, Changsha, China; <sup>4</sup>Department of ENT, Xiangya Third Hospital, Central South University, Changsha, China; <sup>5</sup>Department of ENT, Xiangya Hospital, Central South University, Changsha, China; <sup>6</sup>Department of Pathology, Xiangya Hospital, Central South University, Changsha, China; <sup>7</sup>Department of Clinical Chemistry, Xiangya Hospital, Central South University, Changsha, China; <sup>8</sup>Department of Radiology, West Virginia University, Morgantown, West Virginia, USA; <sup>9</sup>School of Public Health, Central South University, Changsha, China; <sup>10</sup>Center for Molecular Medicine, Xiangya Hospital, Central South University, Changsha, China

The ability of the 10–23 DNAzyme to specifically cleave RNA with high efficiency has fuelled expectation that this agent may have useful applications for targeted therapy. Here, we, for the first time, investigated the antitumor and radiosensitizing effects of a DNAzyme (DZ1) targeted to the Epstein-Barr virus (EBV)-LMP1 mRNA of nasopharyngeal carcinoma (NPC) in patients. Preclinical studies indicated that the DNAzyme was safe and well tolerated. A randomized and double-blind clinical study was conducted in 40 NPC patients who received DZ1 or saline intratumorally, in conjunction with radiation therapy. Tumor regression, patient survival, EBV DNA copy number and tumor microvascular permeability were assessed in a 3-month follow-up. The mean tumor regression rate at week 12 was significantly higher in DZ1 treated group than in the saline control group. Molecular imaging analysis showed that DZ1 impacted on tumor microvascular permeability as evidenced by a faster decline of the  $K^{trans}$  in DZ1-treated patients. The percentage of the samples with undetectable level of EBV DNA copy in the DZ1 group was significantly higher than that in the control group. No adverse events that could be attributed to the DZ1 injection were observed in patients.

Received 23 July 2013; accepted 15 October 2013; advance online publication 10 December 2013. doi:10.1038/mt.2013.257

## INTRODUCTION

Nasopharyngeal carcinoma (NPC), a malignancy arising from the epithelium lining of the posterior nasopharynx, is endemic in Southern China and Southeast Asia, with a striking racial and geographic distribution and has caused very serious health problem

in these areas.<sup>1</sup> Epstein-Barr virus (EBV) is a lymphotropic human gamma herpesvirus which infects more than 90% individuals in the human population and has been implicated in the pathogenesis of several human malignancies including Burkitt's and Hodgkin's lymphomas, gastric carcinoma and NPC.<sup>2,3</sup> EBV infection in NPC is classified as type II latent infection in which only EBV nuclear antigen-1 (EBNA-1), latent membrane protein-1 (LMP1), LMP2, and EBV early RNA (EBER) expressions can be detected.<sup>4</sup> Among these proteins, LMP1 is thought to play a key role in the pathogenesis of NPC.<sup>5–7</sup> LMP1 activates several important signal transduction pathways that include nuclear factor  $\kappa$ B, c-jun N-terminal kinases/c-Jun/activator protein-1, mitogen-activated protein kinases/activating transcription factor, and Janus kinase/signal transducers and activators of transcription protein,<sup>8–11</sup> and causes various downstream pathological changes in cell proliferation, antiapoptosis and metastasis.<sup>12,13</sup> Given the critical role of LMP1 in transformation and apoptosis, suppression of LMP1 would provide a sensible strategy to genetically treat NPC. Indeed, antisense oligonucleotides against LMP1 or EBNA-1 have been shown to inhibit viral oncoprotein expression, induce apoptosis, and sensitize the EBV-positive cells to cytotoxic agents.<sup>14,15</sup> Recently, some studies indicated that the RNA interference against LMP1 exhibited an antiproliferative and antimetastasis effect in LMP1 expressing NPCs.<sup>16,17</sup> These studies support that EBV-encoded LMP1 is a potential molecular target for treatment of EBV-associated carcinomas.

NPC is highly radiosensitive, therefore radiotherapy or radiotherapy combining with chemotherapy are the main treatment strategies. However, both modalities are usually accompanied with complications and the acquired resistance to the effects of radiotherapy has emerged as a significant impediment to effective NPC therapy.<sup>18</sup> Thus, it has been a great challenge to identify biological agents as sensitizers that would restore the apoptotic pathway

The first two authors contributed equally to this work.

**Correspondence:** Lun-Quan Sun, Center for Molecular Medicine, Xiangya Hospital, Central South University, Changsha 410078, China.

E-mail: [luquan.sun@csu.edu.cn](mailto:luquan.sun@csu.edu.cn) or Ya Cao, Cancer Research Institute, Central South University, Changsha 410078, China. E-mail: [ycao98@vip.sina.com](mailto:ycao98@vip.sina.com)

and enhance radiosensitivity for treatment of the EBV-associated NPC. DNazymes are small catalytic DNA that was derived from *in vitro* selection.<sup>19</sup> This enzyme has a number of features, which endow it with tremendous potential for applications both *in vitro* and *in vivo* due to its stability, target site recognition and cleavage. Its ability to cleave almost any RNA sequence with high specificity provided it contains purine-pyrimidine di-nucleotides. The ability of the 10–23 DNzyme to specifically cleave RNA with high efficiency under simulated physiological conditions has fuelled expectation that this agent may have useful therapeutic applications in a gene inactivation strategy.<sup>20,21</sup>

DZ1 is a phosphorothioate-modified “10–23” DNzymes specifically targeted at the LMP1 mRNA.<sup>22</sup> It downregulates the expression of LMP1 in a NPC cells and affected the downstream pathways activated by LMP1, including the nuclear factor  $\kappa$ B pathway. Suppression of the LMP1 expression by the LMP1-targeted DNzyme DZ1 enhanced radiosensitivity both *in vivo* and *in vitro*.<sup>23,24</sup> The radiosensitization of NPC by DZ1 was through inhibiting the binding of nuclear factor  $\kappa$ B to the promoter of ataxia telangiectasia mutated.<sup>25</sup> Together, our experimental data provide a solid basis for the further preclinical and clinical testing of LMP1-targeted DNzymes as potential radiosensitizers for treatment of the EBV-associated carcinomas.

Our hypothesis, tested in this study, was that DZ1 treatment would increase the radiosensitivity of NPC to standard radiotherapy. This clinical study evaluated the safety and short-term efficacy of DZ1 in NPC patients.

## RESULTS

### Preclinical studies of the DNzyme

To determine the *in vivo* efficacy of the LMP1-targeted DZ1, human NPC xenograft model was established and tumor growth was measured by detecting luciferase-expressing CNE1-LMP1 cells. Bioluminescence images of the mice treated with phosphate-buffered saline, oligonucleotide control and DZ1 alone or in combination with radiotherapy are shown in **Figure 1a**. The bioluminescence signal intensity was quantitatively analyzed by measuring the total photon flux (**Figure 1b**). As the tumor grew, the luminescence signal increased in mice treated with phosphate-buffered saline or control oligonucleotide (18- to 20-fold from day 2 to day 18). In contrast, the luciferase signal intensity in mice treated with DZ1 was significantly lower than that in controls at day 18 after injection (only tenfold increase), demonstrating the antitumor efficacy of DZ1 *in vivo*. When DZ1 was given adjuvantly with radiotherapy, the efficacy was improved in comparison with radiotherapy alone, confirming the radiosensitizing effect of DZ1.

The toxicity of the DNzyme was evaluated after i.v. and oral route administration in mice. No morbidity or mortality was observed in any of the groups during the course of the study. All hematology values and biochemistry results from tests of hepatic and renal function were normal (**Supplementary Table S1**). No microscopic lesion that could be attributed to the DNzyme treatment was found in liver, spleen, and kidney in any groups.

After i.v. administration of 100 mg/kg DNzyme, the DNzyme oligonucleotide was extracted from plasma and radio-labeled with <sup>32</sup>P using T4 kinase (**Figure 2**). The plasma disappearance curve for the DNzyme could be described by a

two-compartmental model.<sup>26</sup> The peak plasma concentration of  $24.13 \pm 2.6$   $\mu$ g/ml was achieved in mice. The decrease in plasma concentration of the DNzyme followed a bi-exponential pattern with initial distribution half-life ( $t_{1/2\alpha}$ ) of  $0.18 \pm 0.03$  hour and a terminal half-life ( $t_{1/2\beta}$ ) of  $2.55 \pm 1.0$  hours, and area under the plasma concentration-time curve (AUC) was  $54.17 \pm 9.1$   $\mu$ g·h/ml.

### Participants and treatment in clinical settings

Of 78 participants assessed for eligibility, 40 NPC patients were randomized to one of the two treatment groups and received DZ1 ( $n = 20$ ) or saline ( $n = 20$ ) in conjunction of radiotherapy (**Figure 3b**). Forty subjects were enrolled in Xiangya Hospital in Changsha, China, between March 2007 and December 2008. Primary efficacy end point (tumor regression) was assessed in all subjects at the 3-month time point. The patients in two groups were defined before database lock and unblinding (**Figure 3c**). The baseline participant demographics was comparable (**Table 1**).

### Clinical outcome

To assess the radiosensitizing effect of DZ1 on NPC tumor progression, MRI was performed on all the participants in the study at weeks 0, 3, 6, and 12. The tumor volumes were measured using the program Varian Eclipse (Soma Vision) jointly by two specialists (oncologist and radiologist). For DZ1 treatment group, the mean tumor regression rate at week 12 was significantly higher than that in the saline control group ( $97.78 \pm 5.81\%$  and  $87.78 \pm 15.20\%$  respectively,  $P = 0.038$ ) (**Table 2**).

### EBV copy number

EBV LMP1 is one of the key proteins regulating EBV replication and promoting oncogenesis.<sup>27,28</sup> To indirectly demonstrate that DZ1 inhibited the EBV LMP1 expression in NPC patients, we measured the EBV DNA copy number from the plasma collected from patients weekly for 3 month. In all the patient's samples, there was a progressive decrease in EBV DNA copy number with time, some of which followed the tendency to undetectable level (zero), the others declined to the certain level and remained unchanged (persistent), while in some cases, the EBV DNA copy number was rebounded after their being at a low level (rebound). We defined these three patterns as “zero,” “persistent,” or “rebound” and compared the percentage of these patterns between the DZ1-treated and saline control groups.<sup>29</sup> The percentage of the samples with “zero” in the DZ1 group was significantly higher than that in the control group ( $P = 0.000$ ); the number of “persistent” in the DZ1 group was significantly lower in comparison with the control ( $P = 0.023$ ). The samples with the “rebound” feature was also lower in DZ1 treated patients than in the control, however, a statistically significance was not observed ( $P = 0.185$ ) (**Table 3**). When we analyzed the correlation between the change rate of EBV DNA copy number and tumor regression rate for DZ1 + RT and RT alone groups, it was shown that DZ1 + RT treatments caused a relatively quicker decline in both EBV copy number and the tumor volumes than RT alone (**Supplementary Figure S1**).

### Tumor vasculature permeability

The parameter of  $K^{trans}$  derived from DCE-MRI reflects the condition of tumor microvascular permeability<sup>30</sup> and has been widely

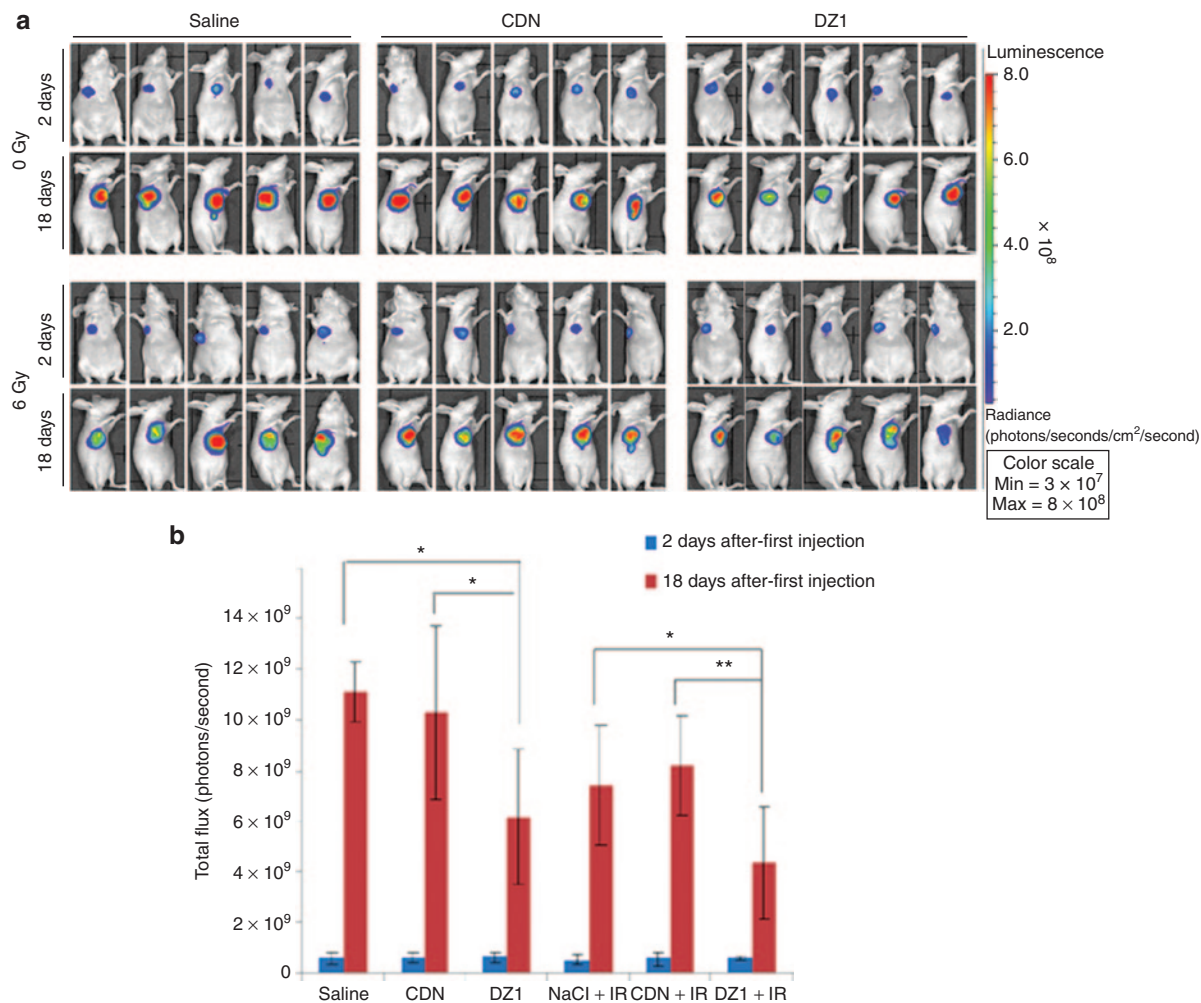


**Figure 1** *In vivo* optical imaging to assess anticancer efficacy of DZ1 with or without radiation therapy (IR) in NPC xenograft model. **(a)** Luciferase-expressing CNE1-LMP1 (CEN-1-LMP1-Luc-DsRED) tumor-bearing mice were monitored by bioluminescence imaging at day 2 and day 18 after first injection. **(b)** *In vivo* average optical signal intensity expressed as photons acquired per second in regions of interest (ROI). Optical signals from the ROI are expressed as mean  $\pm$  SE, \* $P > 0.05$ , \*\* $P > 0.01$ . LMP1, latent membrane protein-1.

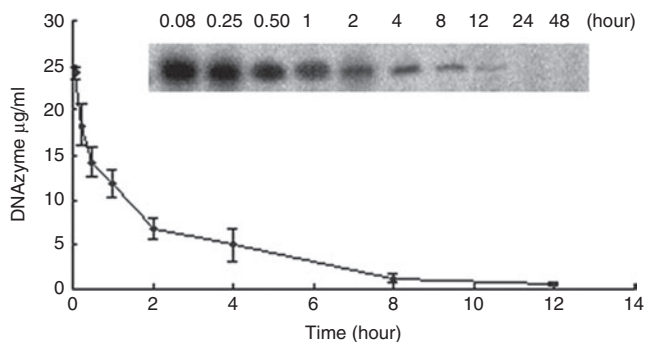


**Figure 2** Plasma concentration versus time after single dose of DNAzyme in mice. Representative autoradiograph showed intact DNAzyme in plasma at various time points after dosing. Plasma concentration-time curve was generated from data in reference to known concentrations of the standard samples. Each point represents mean  $\pm$  SD ( $n = 3$ ).

used for evaluation of antitumor drugs.<sup>31</sup> We compared the  $K^{trans}$  value at the pre-RT with the ones at RT (50 Gy), RT (70 Gy) and 3 months after RT for all the patients. In the DZ1-treated group,

the  $K^{trans}$  value declined gradually, and statistically significant differences of  $K^{trans}$  between pre-RT and three measures during and after RT were observed ( $P = 0.045, 0.004, 0.000$  respectively). For the saline control group,  $K^{trans}$  value also decreased from pre-RT to 3 months after radiotherapy, but, there was no significant difference of the  $K^{trans}$  values of tumor tissues between pre-RT and during RT ( $P = 0.82, 0.4262$ ). Statistically significant difference of the  $K^{trans}$  value only existed between preradiotherapy and 3 months after RT in the saline control patients ( $P = 0.0323$ ) (Table 4). Further comparison between the change rates of  $K^{trans}$  between the DZ1 and saline groups showed a statistically significant difference at the point of 3 months after RT ( $P = 0.03$ ) (Table 4).

**Safety**

There were no adverse events that could be attributed to the DZ1 injection. Blood biochemical analyses were conducted on the blood samples collected from all the participants at week 5 when DZ1 injection completed. Analyses of white blood cell number, hemoglobin concentration, platelet number and lymphocyte cell number showed no significant differences between the DZ1 and

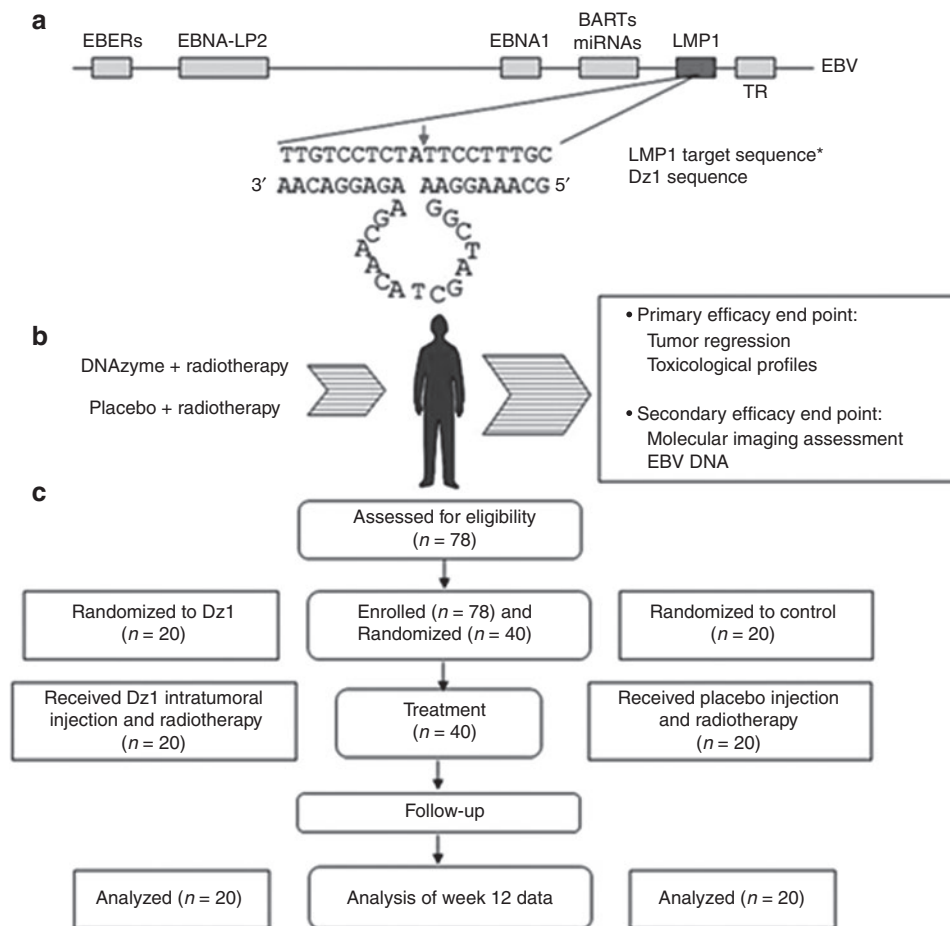


**Figure 3** DNAzyme target site within Epstein-Barr virus (EBV) genome, schematic of protocol design. **(a)** EBV genome is shown together with the target nucleotide sequence and DZ1 sequence (\*GeneBank accession EF419200). The cleavage site is indicated by an arrow. **(b)** This is a schematic of the process. Latent membrane protein-1 (LMP1) positive NPC patients received DZ1 or saline on Monday and Thursday every week in the first 7 weeks, in conjunction with radiotherapy (five times per week from Monday to Friday) and were subjected to assessments in tumor regression, tumor vasculature permeability (molecular imaging analysis), EBV DNA copy numbers and safety evaluation. **(c)** Participant disposition. At screening, a total of 38 patients were excluded; 36 did not meet eligibility criteria and two were excluded for other reasons. Of 40 participants enrolled in the study, none were withdrawn during the course of the study.

control groups (Table 5). Moreover, no abnormal changes in total bilirubin, alanine aminotransferase, aspartate transaminase, blood urea nitrogen, and creatinine were detected (Table 5). Following the Radiation Therapy Oncology Group, the impairment of the skin, mucous membrane and salivary gland that are commonly seen during the radiation therapy was also assessed and analyzed by Wilcoxon rank sum test. No statistical differences were found between two groups, indicating DZ1 treatment did not increase radiation-induced toxicity (Supplementary Table S2).

## DISCUSSION

Use of the nucleic acid-based agents for cancer therapeutics has been explored for decades, which includes antisense oligonucleotides, siRNA and DNAzymes.<sup>20</sup> Due to its unique features in stability and lower cost in manufacturing, DNAzyme has shown its potential in downregulation of the disease genes.<sup>32–34</sup> The present study is, to our knowledge, the first DNAzyme therapy trial conducted to date. Short-term tumor regression (3 months) was significantly lower in the DZ1 treatment group, indicating the antitumor and radiosensitizing effects of DZ1. No safety concerns

associated with DZ1 treatment were identified. All serious adverse events were unrelated to study procedure or study drug injection. Notably, no significant cardiovascular, renal, and hepatic event was reported, indicating that DZ1 is safe. While the current study presents both preclinical and clinical data to show the feasibility of using DZ1 to treat EBV-associated NPC, further DZ1 trials are warranted in a larger patient population with an extended period of time for administration of the DNAzyme and longer follow-up, which may result in a more favorable clinical outcome.

Intratumoral delivery of a therapeutic agent has been attempted in a variety of cancer diseases.<sup>35</sup> These agents consisted of gene therapy approaches, including immunotherapy, oncolytic viral therapy, gene transfer and oligonucleotide-based agents.<sup>36–38</sup> Although NPC lesions tend to be more accessible for intratumoral injection, such an approach is limited by the ability to ensure uniform delivery to the entire lesion. An immuno-liposome encapsulated DZ1 would be stable and targetable for systemic administration with more clinical practicality.

Due to the ethical restrictions to obtain the treated NPC tissues clinically, we did not perform molecular analysis of the DZ1



**Table 1 Characteristics and radiotherapy doses of the study patients<sup>a</sup>**

Characteristics	Distribution		p	
	DZ1	Saline		
Gender	Male	12	16	0.168
	Female	8	4	
Average age	47 (32–60)	49 (29–64)		0.908
T grade	T <sub>1</sub>	0	2	0.207
	T <sub>2</sub>	15	11	
	T <sub>3</sub>	4	3	
	T <sub>4</sub>	1	4	
N grade	N <sub>0</sub>	5	10	0.213
	N <sub>1</sub>	12	9	
	N <sub>2</sub>	3	1	
Clinical stages	II	14	12	0.356
	III	5	4	
	IV	1	4	
Average tumor volume (cm <sup>3</sup> )	17.53	16.93		0.480
Average radiotherapy dosage (Gy)	72.10	73.50		0.500
KPS	88.50	89.00		0.351

EBV, Epstein-Barr virus; KPS, Karnofsky performance status; LMP1, latent membrane protein-1.

<sup>a</sup>The Patients were consecutively enrolled in Xiangya Hospital of Central South University from March 2007 to December 2008. Inclusion criteria are initial treatment patients with poorly differentiated nasopharyngeal squamous carcinoma, EBV LMP1 positive, no distal metastasis, aged between 25 and 65, KPS >70, no radiotherapy taboos, expected life time >3 months and signed Informed Consent Form. Potential patients were excluded if they have any of the followings: serious cardiovascular and cerebrovascular diseases, disorders of lung, hepatic or renal functions, mental diseases and allergic constitution. TNM Classification was adopted by Union for International Cancer Control (2009) <http://www.uicc.org/node/7735>.

**Table 2 Tumor regression rate from DZ1 and saline groups**

Groups	Tumor regression (%) <sup>a</sup>	n	P
DZ1 + RT	97.78 ± 5.81	20	0.038
Saline + RT	86.72 ± 15.20	20	

RT, radiotherapy.

<sup>a</sup>The tumor volumes were derived from MRI measurements 3 months after RT. The rate of tumor regression was calculated using the formula of (pre-RT to 3 months after RT)/pre-RT × 100%.

**Table 3 Distribution of profiles in EBV DNA copy number in DZ1-treated and Control groups<sup>a</sup>**

Patterns	DZ1	Saline	χ <sup>2</sup>	P
Zero	70% (14/20)	15% (3/20)	12.379	0.000
Persistent	5% (1/20)	40% (8/20)	5.161	0.023
Rebound	25% (5/20)	45% (9/20)	1.758	0.185

EBV, Epstein-Barr virus.

<sup>a</sup>The EBV DNA copy number was measured by real-time PCR for patients' plasma (n = 20 for both DZ1 and saline control groups).

effect on the target gene expression. However, the observation of the faster declining in EBV DNA copy number in DZ1-treated patient implied that DZ1 functioned catalytically in suppressing

the EBV LMP1 expression, leading to the inhibition of EBV replication in patients.<sup>28</sup>

As previously established, the EBV LMP1 promoted tumor angiogenesis via directly upregulating vascular endothelial growth factor expression through activating Stat 3 transcriptional factor.<sup>23</sup> Here, we demonstrated that the treatment with LMP1-targeted DZ1 in patients impacted on the tumor microvascular permeability, which implied that the short-term effect of DZ1 in patients may be mediated through the vascular endothelial growth factor pathways.

This study supports our concept that the DZ1 treatment is safe and has efficacy, albeit modest. It shows the potential of DNAzyme therapeutic approach as an adjuvant for radiotherapy for the treatment of cancer and represents a major advance in the field.

## MATERIALS AND METHODS

**Efficacy of DZ1 in NPC xenograft mouse model.** Human NPC cells (CNE1-LMP1) were transduced with Lentiviral vector expressing luciferase and DsRed genes (pLV.ExBi.p/Hygro-EF1a-Luc2-IRES-DsRED-Express2) and selected in Hygromycin. The pooled stable clones of CNE1-LMP1-Luc/DsRed were used for establishment of xenograft model. Athymic Balb/c nude mice (4–6 week, female) were injected subcutaneously with  $1 \times 10^6$  CNE1-LMP1-Luc-DsRED cells (five mice per group). When the tumor volume reached 60–90 mm<sup>3</sup>, the tumor-bearing mice were assigned randomly into six groups: saline control, oligonucleotide control, DZ1 treatment, radiation therapy (IR) + saline, IR + oligonucleotide control and IR + DZ1. A 100 µg of DZ1 or oligonucleotide control were mixed with 2 µl FugeneHD in a total volume of 20 µl in saline. Mice were injected intratumorally every 3 days for six injections. In the groups where the mice were subjected to radiation therapy, one dose of local irradiation at 6 Gy (<sup>60</sup>Co) was given 24 hours after the first DNAzyme injection. Tumor growth was assessed with IVIS II (Caliper Life Sciences, Hopkinton, MA) and the signal intensity of the region of interest was quantitatively analyzed with IGOR-PRO Living Image software (Caliper Life Sciences, Hopkinton, MA).

**Toxicology study.** All the procedures were performed under good laboratory practice conditions. Mice in each group were observed and weighted daily. Blood was collected via retro-orbital sinus puncture once every week, and tissues from humanely euthanized animals were collected. Specimens were processed for clinical pathology, including complete blood count and serum chemistry and histopathology evaluations. A histopathologic assessment was made of sectioned and hematoxylin- and eosin-stained tissues by a board-certified veterinary pathologist.

**Plasma pharmacokinetics.** Plasma pharmacokinetic analysis was performed in BALB/c mice. Mice received injections of 100.0 mg/kg single i.v. dose of DNAzyme oligonucleotide via tail vein. Blood samples were obtained via retro-orbital sinus puncture at 5, 15, and 30 minutes and 1, 2, 4, 8, 12, 24, and 48 hours after administration. DNAzyme oligonucleotide was isolated from plasma samples using the phenol-chloroform extraction method, and was end-labeled with [<sup>32</sup>P]-ATP using T4-polynucleotide kinase and was run on 16% gel electrophoresis. The labeled bands were detected on a phosphor screen and the images were quantitated using the ImageQuant software (GE Healthcare, Milwaukee, WI). The elimination rate constant (β) was calculated from the linear regression analysis of plasma concentration-time curve. The area under the curve (AUC) was calculated using the linear trapezoidal method with extrapolation of the terminal phase to infinity ( $C_{last}/\beta$ ), where  $C_{last}$  is the last measured concentration. Other parameters calculated were: total body clearance ( $Cl$ ) = dose/AUC; volume of distribution ( $Vd$ ) =  $Cl/\beta$ ; and elimination half-life ( $t_{1/2\beta}$ ) =  $0.693/\beta$ .

**DZ1 manufacture.** DZ1 and inactive DNAzyme control (inactive DZ1 with an inverted catalytic core sequence) are 33-mer oligonucleotides

**Table 4**  $K^{\text{trans}}$  derived DCE-MRI from DZ1 and saline control groups

Time points	$K^{\text{trans}}$ (minute <sup>-1</sup> )				change rate of $K^{\text{trans}}$ (%)		
	DZ1	$P^a$	Saline	$P^a$	DZ1	Saline	$P^b$
Pre-RT	0.2048 ± 0.0606		0.1693 ± 0.0619		—	—	
RT (50Gy)	0.1573 ± 0.0605	0.045	0.1652 ± 0.0518	0.8231	-19.71 (-41.96, 11.41)	2.00 (-16.82, 36.73)	0.154
RT (70Gy)	0.1382 ± 0.0671	0.004	0.1414 ± 0.0363	0.4262	-30.24 (-44.50, -19.57)	-6.15 (-14.63, 16.29)	0.078
3 months after RT	0.0862 ± 0.0413	0.000	0.1096 ± 0.0424	0.0323	-52.90 (-68.58, -36.23)	-26.60 (-50.07, 2.56)	0.030

RT, radiotherapy.

<sup>a</sup>Comparison between  $K^{\text{trans}}$  at pre-RT and at RT (50 Gy), RT (70 Gy) and 3 months after RT. <sup>b</sup>Comparison of the  $K^{\text{trans}}$  change rate between DZ1-treated patients and saline-injected patients.

**Table 5** The descriptive statistics and variance analysis of blood chemistry and live or renal function between two groups

Analyses <sup>a</sup>		Readouts			
		DZ1 (n = 20)	Saline (n = 20)	F	P
Blood chemistry	WBC	4.740 ± 1.84	5.660 ± 3.74	1.723	0.197
	Hgb	121.0 ± 11.67	124.0 ± 14.10	0.843	0.364
	PLT	201.4 ± 60.62	224.0 ± 64.11	0.360	0.851
	Lym	0.600 ± 0.55	0.550 ± 0.25	3.010	0.091
Liver and renal function	TBIL	9.22 ± 2.37	9.02 ± 3.22	0.102	0.751
	ALT	20.55 ± 18.83	26.35 ± 15.42	0.244	0.624
	AST	19.74 ± 9.20	24.21 ± 13.03	0.191	0.665
	BUN	4.26 ± 1.32	5.55 ± 2.33	0.561	0.458
	Cr	77.56 ± 11.16	77.73 ± 10.15	0.774	0.385

ALT, alanine aminotransferase; AST, aspartate transaminase; BUN, blood urea nitrogen; Cr, creatinine; Hgb, hemoglobin; Lym, lymphocytes; PLT, platelets; TBIL, total bilirubin; WBC, white blood cells.

<sup>a</sup>The blood samples were taken from patients at the end of DZ1 or saline injections (week 5) and subjected to the tests.

with three phosphorothioate linkages at the 5' and 3' ends (Figure 3a).<sup>22,24</sup> Manufacturing was performed by Oligos Etc (Wilsonville, OR) under good manufacturing practice conditions.

**Patients.** All the participants signed informed consent form after the nature of the study was fully explained. We randomly allocated 40 NPC patients, aged 29–64, to groups either receiving DZ1 or saline. The investigators, site staff, laboratory staff, and patients were blinded to the treatment group assignment.

**Protocol design.** The study recruited participants whose tumor was EBV LMP1 positive as determined by immunohistochemistry. Both groups received radical radiation therapy of 2Gy per time from 6MV-X rays at the frequency of 5 times per week over 7 weeks. DZ1 or saline were injected into tumor under the local anesthetization with the guide of epical endoscope at a dose of 6 mg per injection in 0.1 ml of saline. The DZ1 or saline injections were given 2 hours before radiotherapy twice weekly during the course of radiotherapy.

We performed MRI for tumor progression, X-ray of chest and safety evaluations on all participants who were randomized. We took blood samples throughout the study for analysis of EBV copy number and blood biochemical parameters. We performed DCE-MRI for analysis of tumor vasculature permeability.

**EBV DNA copy number determination.** Concentrations of EBV DNA in plasma were measured using a real-time quantitative PCR system toward the BamHI-W fragment region of the EBV genome. The sequences of the forward and reverse primers were 5'CCCAACTCCACCAC ACC3' and 5'TCTTAGGAGCTGTCCGAGGG3', respectively. A dual

fluorescence-labeled oligomer, 5'(FAM) CA CACTACACACACCCCA CCCGTCTC (TAMRA)3', served as a probe. The real-time quantitative PCR assay (40 cycles) and the reaction-setup procedures have been described in detail previously.<sup>29</sup> Real-time quantitative PCR was performed with the ABI Prism 7700 Sequence Detection Analyzer (Applied Biosystems, Foster City, CA). All DNA samples were also subjected to real-time quantitative PCR for the  $\beta$ -globin gene, which served as a control for the amplifiability of plasma DNA. Multiple negative water blanks were included in every analysis. The EBV and  $\beta$ -globin PCRs were carried out in triplicate. A calibration curve was run in parallel and in duplicate with each analysis, using DNA extracted from an EBV-positive cell line B95-8 (American Type Culture Collection number VR-1492), as a standard. Concentrations of plasma EBV DNA were expressed as the number of copies of the EBV genome per milliliter of plasma. Samples with an undetectable EBV signal after processing under our real-time quantitative PCR conditions (40 cycles) were considered to have zero copies.

**Molecular imaging analysis.** All patients underwent conventional MRI and DCE-MRI scans within 1–2 days before the start of radiotherapy. Subsequent scans were performed during the radiotherapy (radiation dose of 50Gy), at the end of radiotherapy (radiation dose of 70Gy) and 3 months after the end of radiotherapy. MR imaging was performed on a 1.5 T system (MAGNETOM Sonata, Siemens, Germany). For conventional MRI, un-enhanced axial T1-weighted and axial T2-weighted images were obtained. Contrast-enhanced and FAT-suppression T1-weighted images (TR/TE 450/10) were obtained after DCE-MRI scans. DCE-MRI was acquired with TurboFLASH sequence before, during and after bolus i.v. injection of contrast agent (Magnevist; Berlex Laboratories, Wayne, NY). Ten axial sections were selected through the tumor on the basis of T2-weighted imaging. A series of 90 multisection sets were acquired in 360 seconds. At the 6th acquisition, a standard dose (0.2 mmol/kg body weight) bolus of contrast agent was injected via antecubital vein at a rate of 4 ml/second using a contrast agent power injector and then a 20 ml bolus of saline was administered at a rate of 4 ml/second.

The original DCE-MRI data were transferred to an independent workstation and processed using the software NordicICE (Version 2.3.6; Nordic Imaging Lab, Bergen, Norway).<sup>39</sup> First, the arterial input function was semiautomatically obtained from a region of interest (ROI) drawn on the internal carotid artery located in close proximity to the tumor. Second, based on Tofts-kermode two compartment kinetic modeling theory, we performed deconvolution of the tissue response curves (dynamic curves for all pixels) with the arterial input function using the method proposed by Murase.<sup>40</sup> Then, qualitative and quantitative maps of several parameters (such as  $K^{\text{trans}}$ ) related to vascular permeability and intra-extravascular volumes were obtained. For calculating the  $K^{\text{trans}}$  of the tumor, we placed a ROI (diameter of about 9–10 pixels, about 60–70 mm<sup>2</sup> size) on the tumor parenchyma where the  $K^{\text{trans}}$  was the highest.

**Statistical analysis.** For the analyses of efficacy, we predefined two populations who were randomized and received DZ1 or saline. Mean or median values are reported, as appropriate. Comparison between values at various

time points and between values for different variables at the same time point were performed by means of the Wilcoxon signed-rank test for paired data (two-tailed tests). The rate of tumor regression was derived from the tumor volumes from the preradiotherapy (pre-RT) and 3 months after RT. In all analyses, we took statistical significance at the two-sided 5% level, with no adjustment for multiple secondary parameters and analyses.

## SUPPLEMENTARY MATERIALS

**Figure S1.** The correlation between the change rates of EBV DNA copy number and tumor regression rate in patients with (a) radiation therapy (RT) alone or (b) DZ1+RT.

**Table S1.** Effect of DNAzyme administration via i.v. and oral routes on hematological parameters and hepatic and renal function.

**Table S2.** The descriptive statistics and Rank Sum Test of radiation toxicity between two groups.

## ACKNOWLEDGMENTS

We conducted this study in accordance with International Conference on Harmonization-Good Clinical Practice. We obtained approval for the study from Human Ethics Committee of the Xiangya Hospital, Central South University. The approval was also obtained from the Ministry of Science and Technology of China. We thank the patients who enrolled in this study and all the staff and nurses of the Department of Oncology, Xiangya Hospital, Central South University, China. This work was supported by a High-Tec project grant from Ministry of Science and Technology of China (2013BAI01B07), the National Basic Research Program of China (2011CB504300), the National Natural Science Foundation of China (No. 81072220; 81172188) and the "863" National Science and Technology Grants (2009AA02Z403, 2012AA02A501). The authors declared no conflict of interest.

## REFERENCES

- Jemal, A, Bray, F, Center, MM, Ferlay, J, Ward, E and Forman, D (2011). Global cancer statistics. *CA Cancer J Clin* **61**: 69–90.
- Young, LS and Rickinson, AB (2004). Epstein-Barr virus: 40 years on. *Nat Rev Cancer* **4**: 757–768.
- Lo, KW and Huang, DP (2002). Genetic and epigenetic changes in nasopharyngeal carcinoma. *Semin Cancer Biol* **12**: 451–462.
- Pattle, SB and Farrell, PJ (2006). The role of Epstein-Barr virus in cancer. *Expert Opin Biol Ther* **6**: 1193–1205.
- Morris, MA, Dawson, CW and Young, LS (2009). Role of the Epstein-Barr virus-encoded latent membrane protein-1, LMP1, in the pathogenesis of nasopharyngeal carcinoma. *Future Oncol* **5**: 811–825.
- Li, HP and Chang, YS (2003). Epstein-Barr virus latent membrane protein 1: structure and functions. *J Biomed Sci* **10**: 490–504.
- Tsao, SW, Tramoutanis, G, Dawson, CW, Lo, AK and Huang, DP (2002). The significance of LMP1 expression in nasopharyngeal carcinoma. *Semin Cancer Biol* **12**: 473–487.
- Shair, KH, Bendt, KM, Edwards, RH, Bedford, EC, Nielsen, JN and Raab-Traub, N (2007). EBV latent membrane protein 1 activates Akt, NFκB, and Stat3 in B cell lymphomas. *PLoS Pathog* **3**: e166.
- Gires, O, Kohlhuber, F, Kilger, E, Baumann, M, Kieser, A, Kaiser, C et al. (1999). Latent membrane protein 1 of Epstein-Barr virus interacts with JAK3 and activates STAT proteins. *EMBO J* **18**: 3064–3073.
- Eliopoulos, AG, Gallagher, NJ, Blake, SM, Dawson, CW and Young, LS (1999). Activation of the p38 mitogen-activated protein kinase pathway by Epstein-Barr virus-encoded latent membrane protein 1 coregulates interleukin-6 and interleukin-8 production. *J Biol Chem* **274**: 16085–16096.
- Kieser, A, Kilger, E, Gires, O, Ueffing, M, Kolch, W and Hammerschmidt, W (1997). Epstein-Barr virus latent membrane protein-1 triggers AP-1 activity via the c-Jun N-terminal kinase cascade. *EMBO J* **16**: 6478–6485.
- Zhao, Y, Wang, Y, Zeng, S and Hu, X (2012). LMP1 expression is positively associated with metastasis of nasopharyngeal carcinoma: evidence from a meta-analysis. *J Clin Pathol* **65**: 41–45.
- Zheng, H, Li, LL, Hu, DS, Deng, XY and Cao, Y (2007). Role of Epstein-Barr virus encoded latent membrane protein 1 in the carcinogenesis of nasopharyngeal carcinoma. *Cell Mol Immunol* **4**: 185–196.
- Abdulkarim, B, Sabri, S, Zelenika, D, Deutsch, E, Frascogna, V, Klijanienko, J et al. (2003). Antiviral agent cidofovir decreases Epstein-Barr virus (EBV) oncoproteins and enhances the radiosensitivity in EBV-related malignancies. *Oncogene* **22**: 2260–2271.
- Kenney, JL, Guinness, ME, Curiel, T and Lacy, J (1998). Antisense to the Epstein-Barr virus (EBV)-encoded latent membrane protein 1 (LMP-1) suppresses LMP-1 and bcl-2 expression and promotes apoptosis in EBV-immortalized B cells. *Blood* **92**: 1721–1727.
- Mei, YP, Zhou, JM, Wang, Y, Huang, H, Deng, R, Feng, GK et al. (2007). Silencing of LMP1 induces cell cycle arrest and enhances chemosensitivity through inhibition of AKT signaling pathway in EBV-positive nasopharyngeal carcinoma cells. *Cell Cycle* **6**: 1379–1385.
- Li, X, Liu, X, Li, CY, Ding, Y, Chau, D, Li, G et al. (2006). Recombinant adeno-associated virus mediated RNA interference inhibits metastasis of nasopharyngeal cancer cells *in vivo* and *in vitro* by suppression of Epstein-Barr virus encoded LMP-1. *Int J Oncol* **29**: 595–603.
- Lee, AW, Sze, WM, Au, JS, Leung, SF, Leung, TW, Chua, DT et al. (2005). Treatment results for nasopharyngeal carcinoma in the modern era: the Hong Kong experience. *Int J Radiat Oncol Biol Phys* **61**: 1107–1116.
- Santoro, SW and Joyce, GF (1997). A general purpose RNA-cleaving DNA enzyme. *Proc Natl Acad Sci USA* **94**: 4262–4266.
- Zhang, L, Yang, L, Li, JJ and Sun, L (2012). Potential use of nucleic acid-based agents in the sensitization of nasopharyngeal carcinoma to radiotherapy. *Cancer Lett* **323**: 1–10.
- Bhindi, R, Fahmy, RG, Lowe, HC, Chesterman, CN, Dass, CR, Cairns, MJ et al. (2007). Brothers in arms: DNA enzymes, short interfering RNA, and the emerging wave of small-molecule nucleic acid-based gene-silencing strategies. *Am J Pathol* **171**: 1079–1088.
- Lu, ZX, Ye, M, Yan, GR, Li, Q, Tang, M, Lee, LM et al. (2005). Effect of EBV LMP1 targeted DNAzymes on cell proliferation and apoptosis. *Cancer Gene Ther* **12**: 647–654.
- Wang, Z, Luo, F, Li, L, Yang, L, Hu, D, Ma, X et al. (2010). STAT3 activation induced by Epstein-Barr virus latent membrane protein1 causes vascular endothelial growth factor expression and cellular invasiveness via JAK3 And ERK signaling. *Eur J Cancer* **46**: 2996–3006.
- Lu, ZX, Ma, XQ, Yang, LF, Wang, ZL, Zeng, L, Li, ZJ et al. (2008). DNAzymes targeted to EBV-encoded latent membrane protein-1 induce apoptosis and enhance radiosensitivity in nasopharyngeal carcinoma. *Cancer Lett* **265**: 226–238.
- Ma, X, Yang, L, Xiao, L, Tang, M, Liu, L, Li, Z et al. (2011). Down-regulation of EBV-LMP1 radio-sensitizes nasal pharyngeal carcinoma cells via NF-κB regulated ATM expression. *PLoS ONE* **6**: e24647.
- Yu, RZ, Zhang, H, Geary, RS, Graham, M, Masarjian, L, Lemonidis, K et al. (2001). Pharmacokinetics and pharmacodynamics of an antisense phosphorothioate oligonucleotide targeting Fas mRNA in mice. *J Pharmacol Exp Ther* **296**: 388–395.
- Vrzalikova, K, Vockerodt, M, Leonard, S, Bell, A, Wei, W, Schrader, A et al. (2011). Down-regulation of BLIMP1a by the EBV oncogene, LMP-1, disrupts the plasma cell differentiation program and prevents viral replication in B cells: implications for the pathogenesis of EBV-associated B-cell lymphomas. *Blood* **117**: 5907–5917.
- Ahsan, N, Kanda, T, Nagashima, K and Takada, K (2005). Epstein-Barr virus transforming protein LMP1 plays a critical role in virus production. *J Virol* **79**: 4415–4424.
- Lin, JC, Wang, WY, Chen, KY, Wei, YH, Liang, WM, Jan, JS et al. (2004). Quantification of plasma Epstein-Barr virus DNA in patients with advanced nasopharyngeal carcinoma. *N Engl J Med* **350**: 2461–2470.
- Padhani, AR and Leach, MO (2005). Antivascular cancer treatments: functional assessments by dynamic contrast-enhanced magnetic resonance imaging. *Abdom Imaging* **30**: 324–341.
- Cheng, HL (2007). Dynamic contrast-enhanced MRI in oncology drug development. *Curr Clin Pharmacol* **2**: 111–122.
- Zhang, G, Dass, CR, Sumithran, E, Di Girolamo, N, Sun, LQ and Khachigian, LM (2004). Effect of deoxyribozymes targeting c-Jun on solid tumor growth and angiogenesis in rodents. *J Natl Cancer Inst* **96**: 683–696.
- Fahmy, RG, Dass, CR, Sun, LQ, Chesterman, CN and Khachigian, LM (2003). Transcription factor Egr-1 supports FGF-dependent angiogenesis during neovascularization and tumor growth. *Nat Med* **9**: 1026–1032.
- Cairns, MJ, Hopkins, TM, Witherington, C, Wang, L and Sun, LQ (1999). Target site selection for an RNA-cleaving catalytic DNA. *Nat Biotechnol* **17**: 480–486.
- Cross, D and Burmester, JK (2006). Gene therapy for cancer treatment: past, present and future. *Clin Med Res* **4**: 218–227.
- Lai, SY, Koppikar, P, Thomas, SM, Childs, EE, Egloff, AM, Seethala, RR et al. (2009). Intratumoral epidermal growth factor receptor antisense DNA therapy in head and neck cancer: first human application and potential antitumor mechanisms. *J Clin Oncol* **27**: 1235–1242.
- Morgan, RA, Dudley, ME, Wunderlich, JR, Hughes, MS, Yang, JC, Sherry, RM et al. (2006). Cancer regression in patients after transfer of genetically engineered lymphocytes. *Science* **314**: 126–129.
- Bischoff, JR, Kirn, DH, Williams, A, Heise, C, Horn, S, Muna, M et al. (1996). An adenovirus mutant that replicates selectively in p53-deficient human tumor cells. *Science* **274**: 373–376.
- Daldrup-Link, HE, Rydland, J, Helbich, TH, Bjørnerud, A, Turetschek, K, Kvistad, KA et al. (2003). Quantification of breast tumor microvascular permeability with feruglose-enhanced MR imaging: initial phase II multicenter trial. *Radiology* **229**: 885–892.
- Murase, K (2004). Efficient method for calculating kinetic parameters using T1-weighted dynamic contrast-enhanced magnetic resonance imaging. *Magn Reson Med* **51**: 858–862.



This work is licensed under a Creative Commons Attribution-NonCommercial-Share Alike 3.0 Unported License. To view a copy of this license, visit <http://creativecommons.org/licenses/by-nc-sa/3.0/>